Comparing Cyclophellitol N-Alkyl and N-Acyl Cyclophellitol Aziridines as Activity-Based Glycosidase Probes

ARTICLE *in* CHEMISTRY - A EUROPEAN JOURNAL · JUNE 2015

Impact Factor: 5.73 · DOI: 10.1002/chem.201501313 · Source: PubMed

8 AUTHORS, INCLUDING:

Jianbing Jiang

Leiden University

10 PUBLICATIONS **53** CITATIONS

SEE PROFILE

Wouter W Kallemeijn

Leiden University

28 PUBLICATIONS **472** CITATIONS

SEE PROFILE

Hans van den Elst

Leiden University

79 PUBLICATIONS **2,042** CITATIONS

SEE PROFILE

Jeroen D C Codée

Leiden University

114 PUBLICATIONS **2,244** CITATIONS

SEE PROFILE

ChemPubSoc Europe

DOI: 10.1002/chem.201501313

CHEMISTRY
A European Journal
Full Paper

Chemical Biology

Comparing Cyclophellitol *N*-Alkyl and *N*-Acyl Cyclophellitol Aziridines as Activity-Based Glycosidase Probes

Jianbing Jiang, Thomas J. M. Beenakker, Wouter W. Kallemeijn, Gijsbert A. van der Marel, Hans van den Elst, Jeroen D. C. Codée, Johannes M. F. G. Aerts, and Herman S. Overkleeft*[a]

Abstract: The synthesis and evaluation as activity-based probes (ABPs) of three configurationally distinct, fluorescent *N*-alkyl cyclophellitol aziridine isosteres for profiling GH1 β-glucosidase (GBA), GH27 α-galactosidase (GLA) and GH29 α-fucosidase (FUCA) is described. In comparison with the corresponding acyl aziridine ABPs reported previously, the alkyl aziridine ABPs are synthesized easily and are more stable in mild acidic and basic media, and are thus easier to handle. The β-glucose-configured alkyl aziridine ABP proves equally effective in labeling GBA as its *N*-acyl counterpart, whereas the *N*-acyl aziridines targeting GLA and FUCA outperform their *N*-alkyl counterparts. Alkyl aziridines can therefore be an attractive alternative in retaining glycosidase ABP design, but in targeting a new retaining glycosidase both *N*-alkyl and *N*-acyl aziridines are best considered at the onset of a new study.

Introduction

Glycosidases constitute a large family of hydrolytic enzymes expressed throughout all kingdoms of life and are essential in a myriad of biological processes. From a substrate point of view glycosidases can be roughly classified as endoglycosidases (cleaving within an oligo/polysaccharide to yield an oligosaccharide) and exoglycosidases (recognizing a single monosaccharide at the nonreducing end of an oligosaccharide/glycoconjugate). All glycosidases hydrolyze their substrate glycosidic bonds with either retention or inversion of configuration with respect to the anomeric configuration of the released glycoside.[1] This difference in enzymatic hydrolysis, which is perhaps irrelevant with respect to the produced hemiacetals that will undergo posthydrolysis anomerization, is caused by the distinct mechanisms employed by the two enzyme families. Inverting glycosidases directly substitute, in an S_N2 fashion, the aglycon of the glycosidic bond and do so by simultaneously activating the anomeric leaving group (protonation by a catalytic acid/base residue present in the enzyme active site) and activation of a water molecule residing in the active site by a catalytic base. Retaining glycosidases in contrast employ a two-step double displacement mechanism. In this mechanism, first proposed by Koshland,[2] S_N2 displacement of the aglycon (activated through protonation by the general acid/base residue) by attack of the enzyme catalytic nucleophile yields a covalent glycosyl–enzyme intermediate and concomitant expulsion of the aglycon. In a second step and after entry of a water molecule in the enzyme active site this enzyme–glycosyl intermediate is hydrolyzed to yield the carbohydrate hemiacetal.

The occurrence of a covalent intermediate in the catalytic cycle of retaining glycosidases invites the development of tagged, covalent inhibitors, termed activity-based probes (ABPs), and thereby monitoring these enzymes in cell extracts, in situ and in vivo by means of activity-based protein profiling (ABPP) experiments. Indeed, the development of retaining glycosidase ABPs has met with considerable more success than identification of related probes for inverting glycosidases.[3] The first reported conceptual design for retaining glycosidase ABPs is from the laboratories of Withers, Vocadlo and Bertozzi, who employed electron-deficient, fluorine-modified carbohydrates (either substitution of the 2-OH or the 5-H for fluorine).[4] Our work has focused on the natural product mechanism-based β-glucosidase inhibitor, cyclophellitol.[5]

Our first inroads into activity-based glycosidase profiling concerned installment of fluorophores at C6 (glucopyranose numbering) of cyclophellitol.[6] The resulting compounds proved highly potent and very specific for GH1 (CAZypedia nomenclature)[7] human acid glucosylceramidase (GBA) over the other three human retaining β-glucosidases (GBA2, GBA3 and LPH). They also in subsequent studies proved more effective than the corresponding 2-deoxy-2-fluoroglucosides and we resolved to rely on the cyclophellitol scaffold for our ABP design.[8] With the aim to arrive at in-class (with respect to the retaining glycosidase family at hand) broad spectrum ABPs, we substituted the epoxide in cyclophellitol for aziridine and installed the reporter moiety at the aziridine nitrogen through N-acylation. In this fashion we obtained effective ABPs for GH1

[a] *J. Jiang,[+] T. J. M. Beenakker,[+] Dr. W. W. Kallemeijn, Prof. Dr. G. A. van der Marel, H. van den Elst, Dr. J. D. C. Codée, Prof. Dr. J. M. F. G. Aerts, Prof. Dr. H. S. Overkleeft*
Leiden Institute of Chemistry, Leiden University
Einsteinweg 55, 2300 RA Leiden (The Netherlands)
E-mail: h.s.overkleeft@chem.leidenuniv.nl

[+] *These authors contributed equally to this work.*

Supporting information for this article is available on the WWW under http://dx.doi.org/10.1002/chem.201501313.

β-glucosidases,[9] GH27 α-galactosidases (GLA)[10] and GH29 α-fucosidases (FUCA).[11] In each case, as depicted in Figure 1 A, after attack from the catalytic nucleophile present in the glycosidase active site of enzyme, the detectable probe–enzyme complex is formed. Probe specificity appears configuration dependent, with the configuration of cyclitol aziridine conferring selectively towards the corresponding retaining glycosidases.

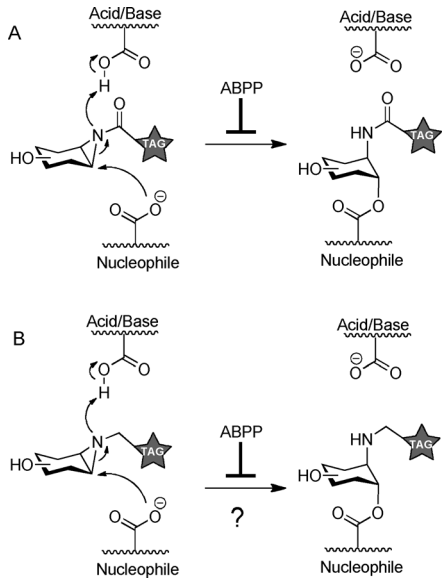

Figure 1. A) Covalent and irreversible inhibition of retaining glycosidases by *N*-acyl cyclophellitol aziridine ABPs. B) Proposed new retaining glycosidase ABP design based on *N*-alkyl cyclophellitol aziridines.

In our studies we observed that *N*-acyl aziridines are relatively hydrolysis-prone, which puts some strain on their synthesis, purification and handling. With the aim of establishing whether *N*-alkyl cyclophellitol aziridines would be valid scaffolds for retaining glycosidase ABP design and following the literature precedent set by Tatsuma and co-workers,[12] we recently evaluated a set of cyclophellitol aziridine analogues varying in N-substitution as inhibitors of human retaining β-glucosidases. We found that *N*-pentenyl cyclophellitol aziridine inhibits GBA, GBA2 and GBA3 at least equally potently as the corresponding *N*-pentenoyl cyclophellitol aziridine.[13] Based on these observations and subject of the here-presented results we embarked on a study in which we compared, side-by-side, the effectiveness (both in synthesis and in ABPP) of the *N*-acyl aziridine probes we reported for GH1 β-glucosidases, GH27 α-galactosidases and GH29 α-fucosidases (Figure 1 A) with their *N*-alkyl counterparts (Figure 1 B). The structures of the compounds studied here and the parent compound cyclophellitol are depicted in Figure 2.

Results and Discussion

The preparation of *N*-acyl cyclophellitol aziridine ABPs **1**, **3** and **5** (Figure 2) is described in our previous reports.[11,14] In order to produce the corresponding *N*-alkyl cyclophellitol aziridines

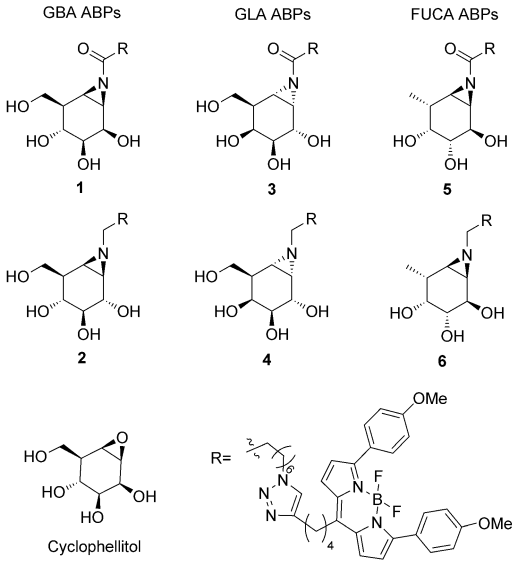

Figure 2. Structures of the natural product, cyclophellitol, and *N*-alkyl/acyl aziridines derived thereof, which are subject of the here-presented studies.

2, **4** and **6** (Scheme 1), we prepared sufficient quantities of the unmodified aziridines **7**, **9** and **11**. These were condensed with 1-azido-8-iodooctane (**13**) in DMF with K_2CO_3 as base, giving azido-aziridine **8**, **10** and **12**. The target ABPs **2**, **4** and **6** were synthesized by conjugation of alkyl-BODIPY **14** followed by HPLC purification and lyophilization in moderate yields.

At a first glance there appears to be not much difference between the efficiency (quantity, yield) of the synthesis of *N*-acyl aziridine **1** (5.8 mg, 6%)[14a] and its alkyl counterpart **2** (26.5 mg, 15%). The same holds true when comparing *N*-acyl

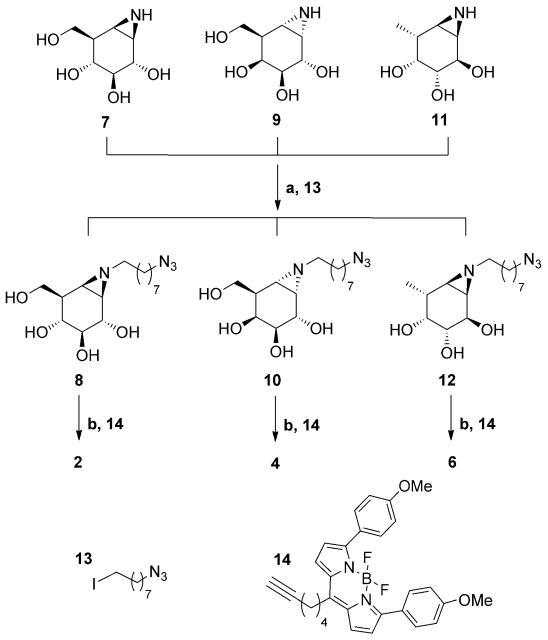

Scheme 1. Synthesis of alkyl aziridine ABPs **2**, **4**, and **6**. a) K_2CO_3, DMF, 80 °C (49% **8**, 24% **10**, 36% **12**); b) $CuSO_4$, sodium ascorbate, DMF (30% **2**, 8% **4**, 9% **6**).

aziridine **3** (7.4 mg, 2%)[14b] and *N*-alkyl aziridine **4** (2.3 mg, 2%) as well as *N*-acylaziridine **5** (15.3 mg, 4%)[11] and *N*-alkyl aziridine **6** (1.8 mg, 3%). However, the HPLC purification of cyclophellitol *N*-acyl aziridines has to be performed at neutral (H_2O, MeCN) or slightly basic (25 mM NH_4HCO_3 in H_2O/MeCN) pH, and hydrolysis of the *N*-acyl aziridine is always at risk during lyophilization and use in ABPP. The *N*-alkyl aziridines in contrast can be purified by standard silica gel column chromatography, and are stable during standard HPLC purification conditions (50 mM aqueous NH_4HCO_3) and LC/MS detection in the presence of 1% TFA, as well as during evaporation or lyophilization.

After obtaining the cyclophellitol aziridine ABPs **1**–**6**, we determined their inhibitory potency towards GBA (**1**, **2**), GLA (**3**, **4**) and FUCA (**5**, **6**) as well as their potential as ABPs for these three retaining glycosidases in a set of head-to-head comparative experiments, focusing in each case on the difference between *N*-acyl- and *N*-alkyl substitution on the cylophellitol aziridines of the same configuration. For this purpose recombinant GBA, GLA and FUCA enzymes were expressed in COS-7 cells.

The first comparative study was performed on acyl aziridine ABP **1** and alkyl aziridine ABP **2** as inhibitors and ABPs of recombinant human acid β-glucoceramidase (GBA). Both aziridines inhibit GBA activity in the nanomolar range, both in vitro and in situ (IC_{50} values in Figure 3A). The observed values for the known *N*-acyl aziridine **1** correspond with those reported previously.[9] Both compounds exhibit a similar pH-dependent activity (Figure 3B) and effective labeling of recombinant purified GBA is observed at concentrations as low as one nanomolar (Figure 3F). Figure 3C depicts a quantification curve of GBA labeling with **1** or **2** as derived from the data presented in Figure 3B offset against GBA-mediated hydrolysis at various pH of the fluorogenic substrate, 4-methylumbelliferyl-β-D-glucopyranoside. These data show that *N*-alkyl-aziridine **2**, as is *N*-acyl-aziridine **1**, is able to covalently modify GBA up to slightly basic conditions, whereas the pH optimum of GBA as reflected by substrate hydrolysis is at around pH 5. Labeling kinetics of *N*-acyl aziridine **1** and *N*-alkyl aziridine **2** at 100 femtomole were determined at both 4 and 37 °C (Figure 3D). Labeling of GBA was almost complete within one minute with both compounds. As shown in Figure 3E, ABPs **1** and **2** have coincident kinetic curves, but effective GBA labeling is too fast to allow accurate determination of kinetic constants. In competitive activity-based protein profiling experiment, we pre-incubated recombinant GBA and wild-type fibroblasts with the mechanism-based inhibitor, conduritol B epoxide (CBE, **15**), the competitive inhibitor, *N*-(adamantanemethyloxypentyl)-deoxynojirimycin (**16**), as well as acyl aziridine (JJB103, **17**) and alkyl aziridine (JJB339, **8**), the latter two compounds being the nonfluorescent precursors towards the synthesis of compounds **1** and **2**, respectively. All compounds proved able to completely block the GBA activity in the conditions applied (Figure 3G). Finally, both **1** and **2** form stable ABP–GBA nucleophile adducts. Labeling intensity of GBA treated with either **1** or **2** did not change after an eight hour chase, which was performed in the dark with hourly continuous extensive washing, and the control adducts were denatured and frozen at −20 °C. Based on these results, we conclude that *N*-alkyl aziridine **2** performs equal to *N*-acyl aziridine **1** in labeling GBA, and is based on the fact that it is easier to prepare and handle, perhaps the retaining β-glucosidase ABP of choice.

The ability of α-galactose-configured cyclophellitol *N*-acyl aziridine **3** and *N*-alkyl aziridine **4** to inhibit and covalently modify recombinant α-galactosidase (rGLA) was established next (Figure 4). Both compounds exhibit nanomolar IC_{50} values both in vitro and in situ (Figure 4A). GLA labeling efficiency by ABP **3** and **4** is pH-dependent, with labeling efficiency of ABP **4** optimal labeling at pH 6.0, and that of ABP **3** at slightly lower pH (Figure 3C). Both probes exhibit optimal labeling close to, but slightly higher than, the pH optimum by which the artificial, fluorogenic GLA substrate 4-methylumbelliferyl-α-galactopyranoside (4-MUαDGal) is hydrolyzed by GLA. From time-course experiments using a 1:1 ratio of enzyme and ABP at 4 or 37 °C, we found that *N*-acyl aziridine **3** labels GLA more efficiently than *N*-alkyl aziridine **4** (Figure 4D and E). GLA labeling by *N*-alkyl aziridine **4** appeared less efficient than with *N*-acyl aziridine **3** (Figure 4F). Labeling with both aziridine **3** and **4** could be competed for by pre-incubation with the nontagged cyclophellitol aziridine **18** as well as with D-galacto-cyclophellitol (**19**)[14b] (Figure 4G). Finally, both *N*-acyl aziridine **3** and *N*-alkyl aziridine **4** formed stable ABP–GLA adducts (Figure 4H). We conclude from these experiments that, *N*-alkyl aziridine **4** is an alternative but less potent ABP than its *N*-acyl counterpart candidate for activity-based profiling of GLA.

In a final set of experiments, recombinant human α-fucosidase (FUCA) was subjected to a similar analysis, using *N*-acyl aziridine **5** and *N*-alkyl aziridine **6**. As can be seen in Figure 5A, *N*-alkyl aziridine **6** inhibits FUCA about 500-fold less potently for than *N*-acyl aziridine **5**. This result is consistent with the detection limit in FUCA labeling with these probes (Figure 5F). FUCA hydrolyses the fluorogenic substrate, 4-methylumbelliferyl-α-L-fucopyranoside (4-MUαFuc, Figure 5C) optimally at pH 5.0, at which pH also optimal labeling with **5** and (though less effective) **6** is observed (Figure 5B). Though a relatively weak mechanism-based inhibitor, the kinetics in FUCA inactivation of *N*-alkyl aziridine **6** could be readily (and more easily than that of the other ABPs subject of this study) determined with $k_i = 98.15\ min^{-1}$ and $K_i' = 87.54\ \mu M$. GBA and GLA labeling kinetics were indeed much more difficult to analyze due to the very fast inhibition rates, compared to FUCA labeling with ABP **6**. This result is backed up by the differences in labeling seen in Figure 5D. *N*-Alkyl aziridine inhibitor JJB349 (**12**) blocked FUCA labeling with either **5** or **6** equally effectively as nontagged *N*-acyl aziridines **20** and **21**. As before, in-gel labeling intensity appeared unchanged between 0 and 8 h of chase (Figure 5H). From these results we conclude that *N*-acyl aziridine ABP **5** is by far the more effective FUCA activity-based probe and the reagent of choice, even though *N*-alkyl aziridine **6** is the most user-friendly in terms of stability and handling.

Conclusions

In conclusion, we have conducted an in-depth study on the efficacy of a new series of *N*-alkyl aziridine-based probes **2**, **4**

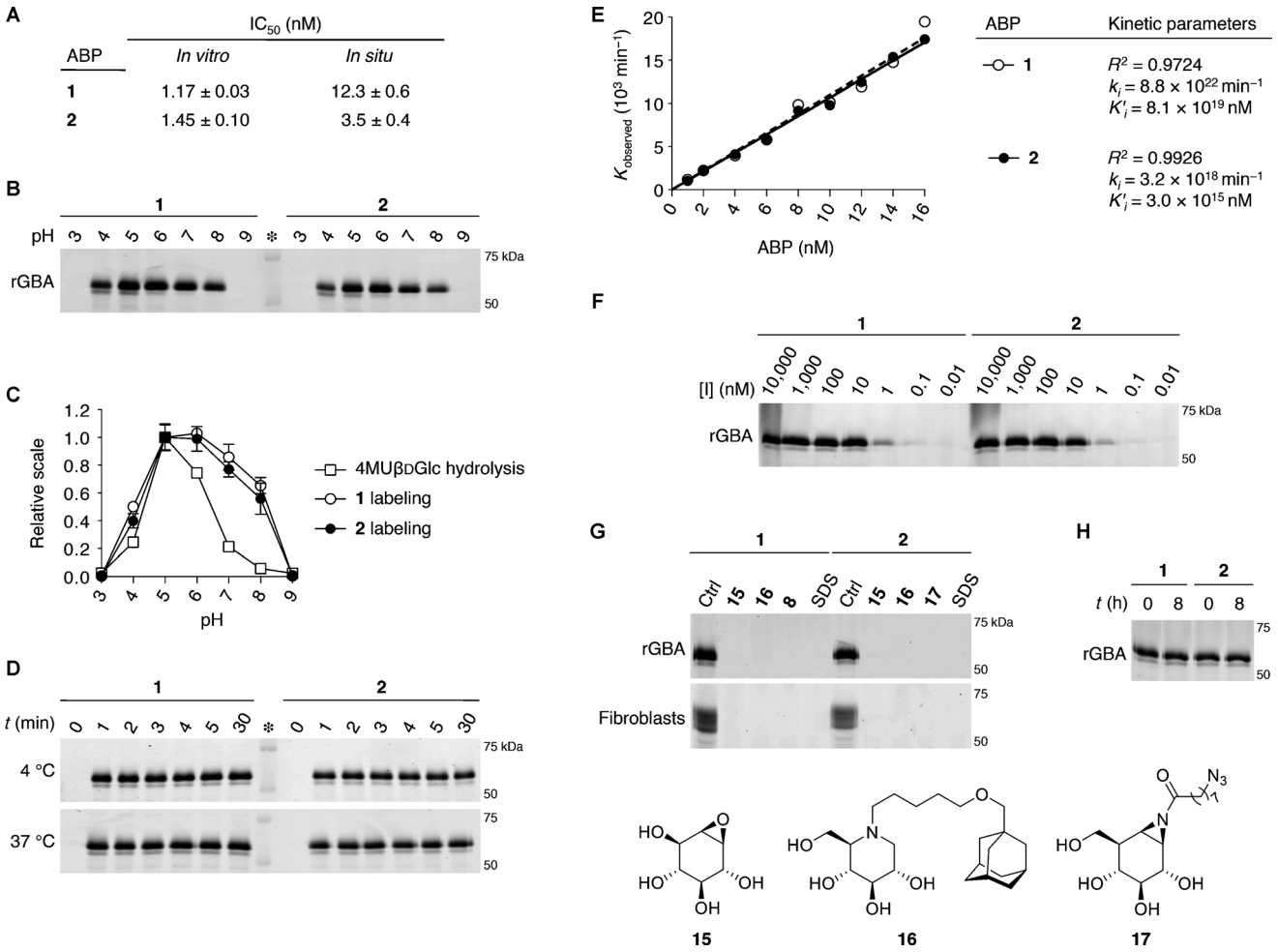

Figure 3. A) Apparent IC_{50} values of β-D-glucopyranose ABPs **1** and **2**, determined in vitro against rGBA and in situ in wild-type GBA fibroblasts. Data average of two separate experiments in duplicate, error bars depict standard deviation. B) ABP-labeling of rGBA at various pH values. C) Quantification of ABP-labeling in (B) compared to hydrolysis of 4-methylumbelliferyl-β-D-glucopyranoside at varying pH values. D) Labeling of 100 fmol rGBA with 100 fmol ABP at 4 °C (top) and 37 °C (bottom). E) Determination of inhibition constants. The graph depicts $K_{obs.}$ against [ABP]; the table shows the kinetic parameters k_i and K_i' estimated with one-phase exponential association. Data average of two separate experiments in duplicate, error bars depict standard deviation. F) Detection limit of ABP-emitted fluorescence. rGBA (10 pmol) was labeled with varying concentrations of ABP **1** or **2**. G) ABP labeling of rGBA (top) or wild-type GBA fibroblast lysate (bottom) competed with inhibitors **8** (Scheme 1), **15**, **16**, **17**, or SDS. H) Stability of ABP–rGBA nucleophile adducts after a 0 and 8 h chase in the dark, with hourly extensive washing.

and **6** as activity-based probes for retaining glycosidases. We compared the efficacy of these probes—relatively easy to synthesize and handle—with our previously reported set of *N*-acyl aziridine probes **1**, **3** and **5**, which we developed for the profiling of GBA, GLA and FUCA, respectively. Preparation of alkyl aziridine compounds is easier because of the intrinsically more stable (compared to *N*-acyl aziridines) *N*-alkyl aziridine electrophilic trap. Activity-based labeling of GBA proved equally effective with *N*-alkyl aziridine **2** as with *N*-acyl aziridine acyl **1**, but the corresponding *N*-alkyl analogues for GLA and especially FUCA proved to perform less well. These intriguing results warrant future investigations using crystals of the various retaining glycosidases soaked with corresponding ABPs to render an explanation. We thus conclude that *N*-alkyl aziridines can be considered as scaffold to design activity-based probes directed at retaining glycosidases other than targeted to date, but when not active the corresponding *N*-acyl derivatives need be assessed as well before disregarding the cyclophellitol scaffold for ABPP targeting of the glycosidase at hand.

Experimental Section

General synthesis

All reagents were of a commercial grade and were used as received unless stated otherwise. Dichloromethane (DCM), tetrahydrofuran (THF) and *N*,*N*-dimethylformamide (DMF) were stored over 4 Å molecular sieves, which were dried in vacuo before use. All reactions were performed under an argon atmosphere unless stated otherwise. Solvents used for flash column chromatography were of pro-analysis quality. Reactions were monitored by TLC analysis using Merck aluminium sheets precoated with silica gel 60 with detection by UV absorption (254 nm) and by spraying with a solution of $(NH_4)_6Mo_7O_{24}{\cdot}H_2O$ (25 g L^{-1}) and $(NH_4)_4Ce(SO_4)_4{\cdot}H_2O$ (10 g L^{-1}) in 10% sulfuric acid, followed by charring at approxi-

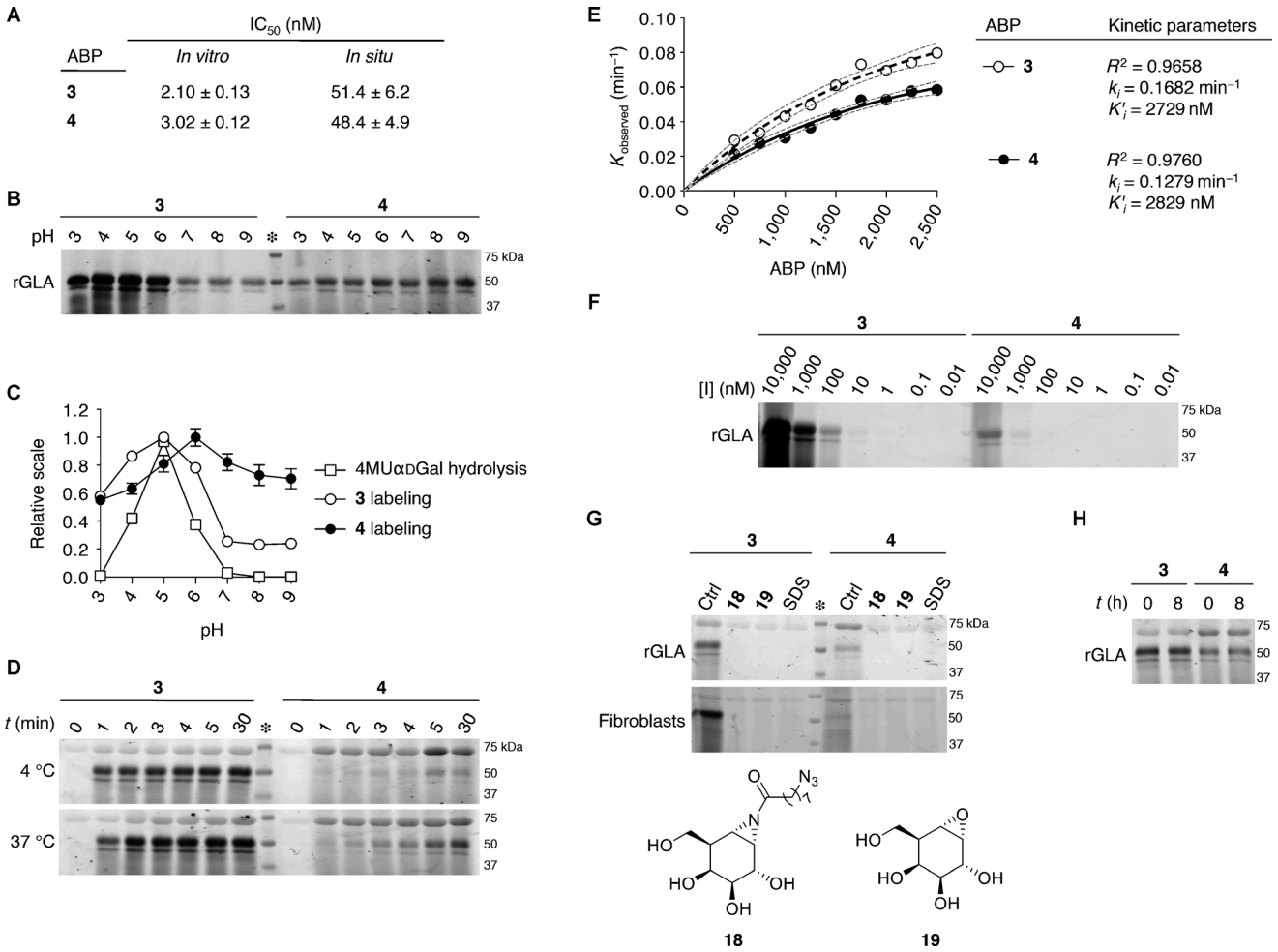

Figure 4. A) Apparent IC_{50} values of α-galactopyranose ABPs **3** and **4**, determined in vitro against rGLA and in situ in wild-type GLA fibroblasts. Data average of two separate experiments in duplicate, error bars depict standard deviation. B) ABP-labeling of rGLA at varying pH values. C) Quantification of ABP-labeling in (B) compared to hydrolysis of 4-methylumbelliferyl-α-galactopyranoside at various pH values. D) Labeling of 100 fmol rGLA with 100 fmol ABP at 4 °C (top) and 37 °C (bottom). E) Determination of inhibition constants. The graph depicts $K_{obs.}$ against [ABP]; the table shows the kinetic parameters k_i and K_i' estimated with one-phase exponential association. Data average of two separate experiments in duplicate, error bars depict standard deviation. F) Detection limit of ABP-emitted fluorescence. rGLA (10 pmol) was labeled with varying concentrations of ABP. G) ABP labeling of rGLA (top) or wild-type GLA fibroblast lysate (bottom) competed with the inhibitor **18**, or **19** or SDS. H) Stability of ABP–rGLA nucleophile adducts after a 0 and 8 h chase in the dark, with hourly extensive washing.

mately 150 °C or by spraying with an aqueous solution of $KMnO_4$ (7%) and K_2CO_3 (2%) followed by charring at about 150 °C. Column chromatography was performed using either Baker or Screening Device silica gel 60 (0.04–0.063 mm) in the indicated solvents. ^1H and ^{13}C NMR spectra were recorded on Bruker AV-850 (850/214 MHz), Bruker DMX-600 (600/150 MHz) and Bruker AV-400 (400/100 MHz) spectrometer in the given solvent. Chemical shifts are given in ppm relative to the chloroform residual solvent peak or tetramethylsilane (TMS) as internal standard. Coupling constants are given in Hz. All given ^{13}C spectra are proton decoupled. High-resolution mass spectra were recorded with a LTQ Orbitrap (Thermo Finnigan). FT-IR spectra were recorded on a Shimadzu FT-IR 83000 spectrometer. LC/MS analysis was performed on an LCQ Adventage Max (Thermo Finnigan) ion-trap spectrometer (ESI^+) coupled to a Surveyor HPLC system (Thermo Finnigan) equipped with a C_{18} column (Gemini, 4.6 mm × 50 mm, 3 μm particle size, Phenomenex) equipped with buffers A: H_2O, B: acetonitrile (MeCN), and C: 1% aqueous TFA. For reversed-phase HPLC purifications an Agilent Technologies 1200 series instrument equipped with a semipreparative Gemini C_{18} column (10 × 250 mm) was used. The applied buffers were A: 50 mM NH_4HCO_3 in H_2O, B: MeCN.

Synthesis and characterization of compounds 1–21

The β-D-glucoside acyl β-aziridine ABPs JJB75 (**1**) and JJB103 (**17**) were synthesized as described earlier.[9] CBE **15** was bought from Sigma and iminosugar **16** was synthesized as reported before.[15] The α-D-galactoside α-epoxide compound LWA481 (**19**), LWA491 (**3**) and acyl α-aziridines LWA468 (**18**) were synthesized as described earlier.[10] The α-L-fucoside acyl α-aziridines JJB244 (**5**), JJB237 (**20**) and JJB261 (**21**) were synthesized as described earlier.[11]

8: Unprotected cyclophellitol aziridine **7**[14a] (163 mg, 0.93 mmol, 1.0 equiv) was dissolved in DMF (4 mL). Compound **13**, 1-azido-8-iodooctane (360 mg, 1.28 mmol, 1.38 equiv) and K_2CO_3 (448 mg, 4.0 mmol, 4.3 equiv) were added to the solution and the mixture was stirred at 80 °C for 24 h. After the full conversion of the starting material, the resulting solution was filtered over a pad of Celite

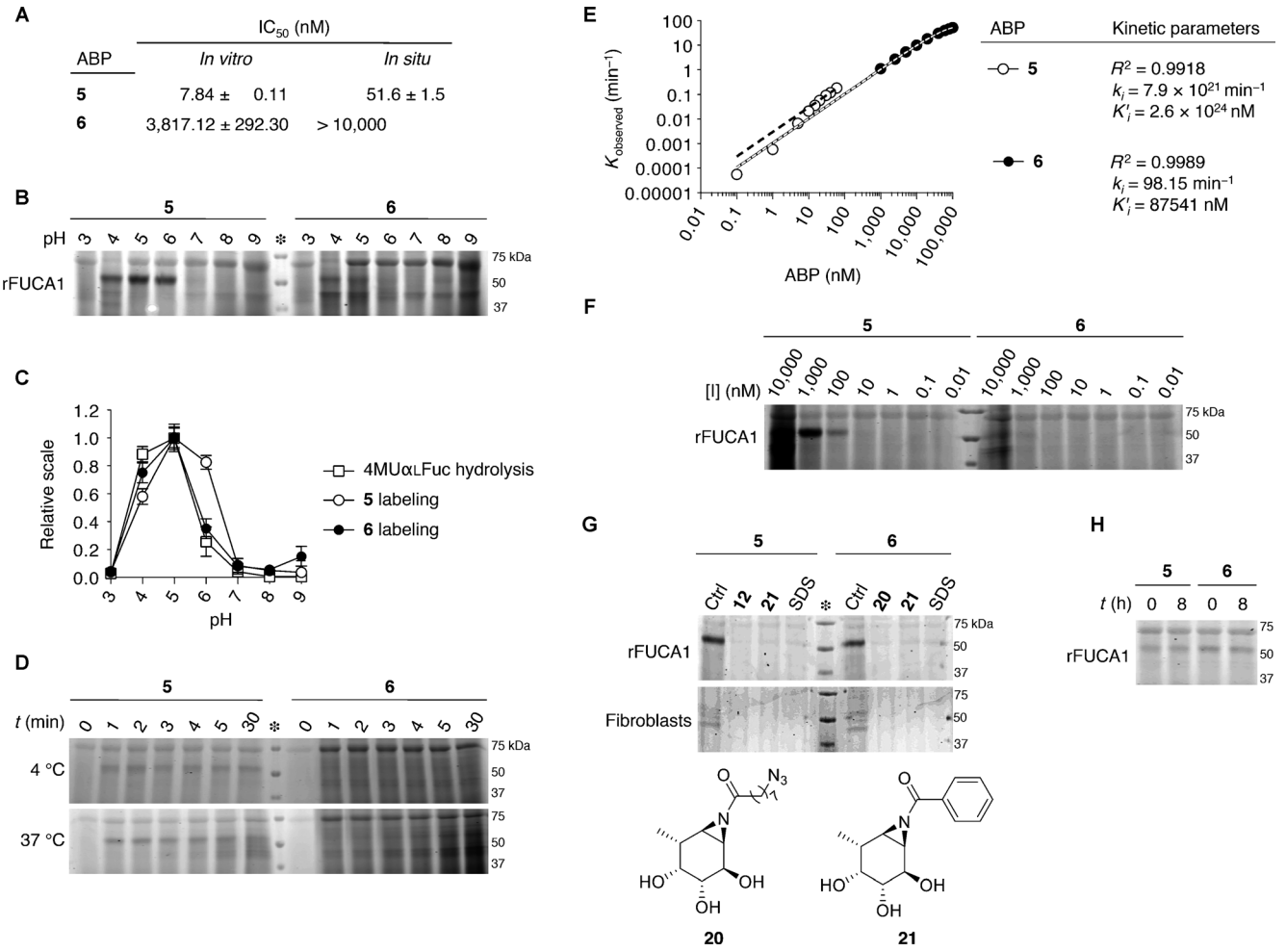

Figure 5. A) Apparent IC_{50} values of α-L-fucopyranose ABPs **3** and **4**, determined in vitro against rFUCA and in situ in wild-type FUCA fibroblasts. Data average of two separate experiments in duplicate, error bars depict standard deviation. B) ABP-labeling of rFUCA at varying pH. C) Quantification of ABP-labeling in (B) compared to hydrolysis of 4-methylumbelliferyl-α-L-fucopyranoside at varying pH values. D) Labeling of 100 fmol rFUCA with 100 fmol ABP at 4 °C (top) and 37 °C (bottom). E) Determination of inhibition constants. Graph depicts $K_{obs.}$ against [ABP]; the table shows the kinetic parameters k_i and K_i' estimated with one-phase exponential association. Data average of two separate experiments in duplicate, error bars depict standard deviation. F) Detection limit of ABP-emitted fluorescence. rFUCA (10 pmol) was labeled with varying concentrations of ABP. G) ABP labeling of rFUCA (top) or wild-type FUCA fibroblast lysate (bottom) competed with the irreversible inhibitors **12** (Scheme 1), **20**, or **21** or SDS. H) Stability of ABP–rFUCA nucleophile adducts after a 0 and 8 h chase in the dark, with hourly extensive washing.

in syringe and the volatiles were concentrated under reduced pressure. Then the crude product was purified by silica gel column chromatograph (linear gradient: 2→20%, MeOH in DCM) resulting as a colorless oil **8** (150 mg, 0.46 mmol, 49%). TLC: $R_f = 0.41$ (15%, v/v, MeOH in DCM); $[\alpha]_D^{20} = +49.6$ ($c = 1$, MeOH); ^{1}H NMR (400 MHz, CD_3OD): $\delta = 3.99$ (dd, $J = 11.3$, 4.5 Hz, 1H), 3.66–3.59 (m, 2H), 3.28 (t, $J = 8.0$ Hz, 2H), 3.15–3.02 (m, 2H), 2.40–2.33 (m, 1H), 2.18–2.11 (m, 1H), 2.01–1.98 (m, 1H), 1.95–1.85 (m, 1H), 1.66 (d, $J =$ 6.2 Hz, 1H), 1.62–1.52 (m, 4H), 1.44–1.27 ppm (d, $J = 13.6$ Hz, 8H); ^{13}C NMR (101 MHz, CD_3OD): $\delta = 78.92$, 73.79, 70.15, 63.76, 62.05, 52.40, 45.36, 45.34, 42.98, 30.45, 30.24, 30.14, 29.85, 28.25, 27.72 ppm; IR (film): $\tilde{\nu} = 3316$, 2926, 2855, 2095, 1454, 1348, 1256, 1096, 1020, 818 cm^{-1}; LC/MS analysis: $t_R = 4.41$ min (linear gradient 10→90% B in 12.5 min), *m/z* 329.20 $[M+H]^+$; HRMS: calcd for $C_{15}H_{28}N_4O_4$ $[M+H^+]$ 329.21833, found: 329.21809.

2: Azide compound **8** (36.0 mg, 0.109 mmol, 1 equiv) was dissolved in DMF (3 mL), red BODIPY compound **14** (52.7 mg, 0.11 mmol, 1.1 equiv), $CuSO_4$ (1 M, 60 μL, 0.060 mmol, 0.55 equiv) and sodium ascorbate (1 M, 70 μL, 0.070 mmol, 0.64 equiv) was added to the solution under argon atmosphere. After stirring at room temperature, overnight, the resulting mixture was concentrated under reduced pressure. Then the crude product was purified by semipreparative reversed HPLC (linear gradient: 50→56% B in A, 12 min, solutions used A: 50 mM NH_4HCO_3 in H_2O, B: MeCN) and lyophilized resulting as a purple powder product **2** (26.5 mg, 0.032 mmol, 30%). ^{1}H NMR (400 MHz, CD_3OD): $\delta = 7.86$–7.81 (m, 4H), 7.63 (s, 1H), 7.41 (d, $J = 4.4$ Hz, 2H), 7.00–6.91 (m, 4H), 6.68 (d, $J = 4.4$ Hz, 2H), 4.29 (t, $J = 7.0$ Hz, 2H), 3.99 (dd, $J = 10.0$, 4.4 Hz, 1H), 3.83 (s, 6H), 3.62–3.57 (m, 2H), 3.13–3.08 (m, 1H), 3.03–2.98 (m, 3H), 2.75 (t, $J = 6.7$ Hz, 2H), 2.32–2.25 (m, 1H), 2.10–2.01 (m, 1H), 1.97–1.94 (m, 1H), 1.90–1.78 (m, 7H), 1.62 (d, $J = 6.3$ Hz, 1H), 1.55–1.45 (m, 2H), 1.35–1.15 ppm (m, 8H); ^{13}C NMR (101 MHz, CD_3OD): $\delta = 162.18$, 158.75, 148.58, 146.75, 137.48, 132.15, 128.44, 126.49, 123.23, 121.05, 114.64, 79.02, 73.89, 70.12, 63.78, 62.09, 55.83, 51.22, 45.50, 45.42, 43.01, 34.14, 31.22, 30.97, 30.34, 30.23, 29.87, 28.16, 27.34, 25.77 ppm; LC/MS analysis: $t_R = 6.85$ min (linear gradient 10→90% B in 12.5 min), *m/z* 813.27 $[M+H]^+$; HRMS: calcd for $C_{44}H_{55}BF_2N_6O_6$ $[M+H^+]$ 813.43245, found: 813.43125.

10: Unprotected cyclophellitol aziridine **9**[14b] (87.6 mg, 0.50 mmol, 1.0 equiv) was dissolved in DMF (4 mL). Compound **13**, 1-azido-8-iodooctane (224 mg, 0.80 mmol, 1.3 equiv) and K_2CO_3 (297 mg, 2.15 mmol, 4.3 equiv) were added to the solution and the mixture was stirred at 80 °C for 18 h. After the full conversion of the starting material, the resulting solution was concentrated under reduced pressure. Then the crude product was purified by silica gel column chromatography (linear gradient: 3→20%, MeOH in DCM) resulting as a colorless oil **10** (40 mg, 0.121 mmol, 24%). TLC: R_f = 0.3 (10%, v/v, MeOH in DCM); ^{1}H NMR (850 MHz, CD_3OD): δ = 4.02 (dd, J = 4.3, 8.5 Hz, 1H), 3.79–3.77 (m, 1H), 3.76–3.73 (m, 1H), 3.70–3.68 (m, 1H), 3.33 (dd, J = 8.5, 1.7 Hz 1H), 3.27 (t, J = 4.0 Hz, 2H), 2.38–2.34 (m, 1H), 2.20–2.16 (m, 1H), 1.94 (dd, J = 6.8, 4.3 Hz, 1H), 1.91–1.88 (m, 1H), 1.61–1.57 (m, 4H), 1.55 (d, J = 6.8 Hz, 1H), 1.41–1.31 ppm (m, 8H); ^{13}C NMR (214 MHz, CD_3OD): δ = 74.94, 73.24, 70.44, 63.38, 62.40, 52.48, 46.24, 44.89, 42.21, 30.59, 30.47, 30.17, 29.90, 28.36, 27.77 ppm; LC/MS analysis: t_R = 5.47 min (linear gradient 10→50% B in 12.5 min), m/z 329.20 $[M+H]^+$; HRMS: calcd for $C_{15}H_{28}N_4O_4$ $[M+H^+]$ 329.21833, found: 329.21815.

4: Azide compound **10** (12.0 mg, 0.036 mmol, 1 equiv) was dissolved in DMF (2 mL), red BODIPY compound **14** (20.9 mg, 0.043 mmol, 1.2 equiv), $CuSO_4$ (1 M, 13 μL, 13 μmol, 0.36 equiv) and sodium ascorbate (1 M, 14 μL, 14 μmol, 0.39 equiv) were added to the solution under argon atmosphere. After stirring at room temperature for 18 h, the resulting mixture was concentrated under reduced pressure. Then the crude product was purified by semipreparative reversed HPLC (linear gradient: 52→60% B in A, 12 min, solutions used A: 50 mM NH_4HCO_3 in H_2O, B: MeCN) and lyophilized resulting as a purple powder product **4** (2.3 mg, 2.8 μmol, 8%). ^{1}H NMR (850 MHz, CD_3OD): δ = 7.86–7.83 (m, 4H), 7.70 (s, 1H), 7.44 (d, J = 7.44 Hz, 2H), 6.99 −6.96 (m, 4H) 6.70 (d, J = 4.3 Hz, 2H), 4.33 (t, J = 6.8 Hz, 2H), 4.00 (dd, J = 8.5, 4.3 Hz, 1H), 3.85 (s, 6H), 3.78–3.76 (m, 1H), 3.75–3.72 (m, 1H), 3.69–3.67 (m, 1H), 3.33–3.32 (m, 1H), 3.07 (t, J = 7.7 Hz, 2H), 2.79 (t, J = 6.8 Hz, 2H), 2.30–2.27 (m, 1H), 2.14–2.10 (m, 1H), 1.90–1.82 (m, 8H), 1.55–1.49 (m, 3H), 1.31–1.21 ppm (m, 8H); ^{13}C NMR (214 MHz, CD_3OD): δ = 162.19, 158.79, 146.77, 137.48, 132.16, 128.44, 126.50, 121.03, 114.63, 74.88, 73.16, 70.37, 63.33, 62.31, 55.90, 55.83, 52.25, 46.19, 44.84, 42.14, 34.14, 31.24, 30.97, 30.44, 30.40, 30.34, 29.87, 28.21, 27.35, 25.78 ppm; LC/MS analysis: t_R = 6.76 min (linear gradient 10→90% B in 12.5 min), m/z 813.33 $[M+H]^+$; HRMS: calcd for $C_{44}H_{55}BF_2N_6O_6$ $[M+H^+]$ 813.43245, found 813.43237.

12: Unprotected aziridine compound **11**[11] (44 mg, 0.28 mmol, 1 equiv) was dissolved in DMF (2 mL). Compound **13**, 1-azido-8-iodooctane (118 mg, 0.42 mmol, 1.5 equiv) and K_2CO_3 (174 mg, 1.26 mmol, 1.38 equiv) were added to the solution and the mixture was stirred at 80 °C for 24 h. After the full conversion of the starting material, the resulting solution was filtered over a pad of Celite in syringe and the volatiles were concentrated under reduced pressure. Then the crude product was purified by silica gel column chromatograph (linear gradient: 0→10%, MeOH in DCM) resulting as a colorless oil **12** (31 mg, 0.10 mmol, 36%). TLC: R_f = 0.39 (10%, v/v, MeOH in DCM); $[\alpha]_D^{20}$ = −47.6 (c = 0.5, MeOH); ^{1}H NMR (850 MHz, CD_3OD): δ = 3.99 (dd, J = 8.7, 4.3 Hz, 1H), 3.54–3.53 (m, 1H), 3.34 (dd, J = 9.4, 7.5 Hz, 1H), 3.28 (t, J = 6.9 Hz, 2H), 2.37–2.34 (m, 1H), 2.15–2.12 (m, 1H), 1.91–1.89 (m, 1H), 1.87–1.86 (m, 1H), 1.61–1.57 (m, 4H), 1.40–1.33 (m, 9H), 1.16 ppm (d, J = 7.5 Hz, 3H); ^{13}C NMR (214 MHz, CD_3OD): δ = 76.05, 75.13, 70.18, 62.33, 52.45, 46.45, 45.76, 36.95, 30.60, 30.57, 30.18, 29.89, 28.32, 27.75, 16.75 ppm; IR (film): $\tilde{\nu}$ = 3370, 2927, 2854, 2092, 1456, 1348, 1253, 1105, 1057, 814, 748 cm^{-1}; LC/MS analysis: t_R = 5.06 min (linear gradient 10→90% B in 12.5 min), m/z 313.20 $[M+H]^+$; HRMS: calcd for $C_{15}H_{28}N_4O_3$ $[M+H^+]$ 313.22342, found: 313.22387.

6: Azide compound **12** (8.30 mg, 0.0266 mmol, 1 equiv) was dissolved in DMF (0.8 mL). Red BODIPY **14** (13.0 mg, 0.033 mmol, 1.24 equiv), $CuSO_4$ (1 M, 12 μL, 0.012 mmol, 0.45 equiv) and sodium ascorbate (1 M, 13 μL, 0.013 mmol, 0.48 equiv) were added to the solution under argon atmosphere. After being stirred at room temperature for 12 h, the reaction volatiles were removed under reduced pressure. Then the crude product was purified by semipreparative reversed HPLC (linear gradient: 58→68% B in A, 12 min, solutions used A: 50 mM NH_4HCO_3 in H_2O, B: MeCN) and lyophilized to give a purple powder product **6** (1.84 mg, 2.31 μmol, 9%). ^{1}H NMR (600 MHz, CD_3OD): δ = 7.86–7.83 (m, 4H), 7.69 (s, 1H), 7.43 (d, J = 4.4 Hz, 2H), 6.98–6.96 (m, 4H), 6.69 (d, J = 4.3 Hz, 2H), 4.33 (t, J = 7.0 Hz, 2H), 3.99 (dd, J = 8.7, 4.3 Hz, 1H), 3.85 (s, 6H), 3.52–3.51 (m, 1H), 3.34–3.32 (m, 1H) 3.06 (t, J = 7.3 Hz, 2H), 2.78 (t, J = 6.8 Hz, 2H), 2.28–2.24 (m, 1H), 2.10–2.05 (m, 1H), 1.89–1.82 (m, 7H), 1.52–1.48 (m, 2H), 1.31–1.21 (m, 9H), 1.13 ppm (d, J = 7.5 Hz, 3H); ^{13}C NMR (151 MHz, CD_3OD): δ = 162.18, 158.76, 146.75, 137.48, 132.15, 128.42, 126.49, 123.25, 121.00, 114.61, 76.03, 75.08, 70.11, 62.26, 55.81, 51.24, 46.44, 45.69, 36.91, 34.13, 31.24, 30.96, 30.53, 30.45, 30.32, 29.91, 28.20, 27.34, 25.75, 16.79 ppm; LC/MS analysis: t_R = 6.96 min (linear gradient 10→90% B in 12.5 min), m/z 797.07 $[M+H]^+$; HRMS: calcd for $C_{44}H_{55}BF_2N_6O_5$ $[M+H^+]$ 796.44041, found: 796.44218.

Materials of biological assays

Recombinant GBA and GLA were obtained from Genzyme (Cambridge, MA, USA). Fibroblast cell lines containing wild-type GBA, GLA and FUCA1 were cultured in HAMF12-DMEM medium (Invitrogen) supplied with 10% (v/v).

Molecular cloning and recombinant expression

Confluent COS-7 cells were transfected with pcDNA3.1 empty vector (mock) or vector containing the coding sequence of *H. sapiens* FUCA1 (NCBI reference sequence XM_005245821.1; cloning described in conjunction with FuGENE (Roche).[11] After 72 h, cells were harvested by scraping in potassium phosphate buffer (25 mM K_2HPO_4/KH_2PO_4, pH 6.5, supplemented with 0.1% (v/v) Triton X-100 and protease inhibitor cocktail (Roche)). After determination of the protein concentration (BCA kit, Pierce), lysates were transferred to aliquots and frozen at −80 °C.

Enzyme activity assays and IC_{50} measurements

The β-D-glucosidase activity of rGBA was assayed at 37 °C by incubating with 3.75 mM 4-methylumbelliferyl-β-D-glucopyranoside as substrate in 150 mM McIlvaine buffer, pH 5.2, supplemented with 0.2% (w/v) sodium taurocholate, 0.1% (v/v) Triton X-100 and 0.1% (w/v) BSA. The α-D-galactosidase activity of rGLA was assayed using 3.0 mM 4-methylumbelliferyl-α-D-galactopyranoside in 150 mM McIlvaine buffer, pH 4.6, supplemented with 0.1% (w/v) BSA. The α-L-fucosidase activity of rFUCA1 was determined by incubating with 1.5 mM 4-methylumbelliferyl-α-L-fucopyranoside in 150 mM McIlvaine buffer, pH 5.0, supplemented with 0.1% (w/v) BSA. The values obtained correspond to net α-L-fucosidase activity left after subtraction of endogenous α-L-fucosidase activity present in lysate of mock-transfected COS-7 cells. To determine the apparent in vitro IC_{50} value, recombinant GBA, GLA or lysate of COS-7 cells, either mock or over-expressing FUCA1, was firstly pre-incubated with a range of inhibitor dilutions for 30 min at 37 °C, prior to addition of the substrate. To determine the influence of pH on the enzymatic activity, enzyme mixtures were firstly pre-incubated for 30 min on ice with McIlvaine buffers of pH 3–9 after which sub-

strate was added, dissolved in Nanopure H_2O. The enzymatic reaction was quenched by adding excess NaOH/glycine (pH 10.6), after which fluorescence of liberated 4-methylumbelliferyl was measured with a fluorimeter LS55 (PerkinElmer) using $\lambda_{EX}=366$ nm and $\lambda_{EM}=445$ nm. The in situ IC_{50} value was determined by incubating confluent fibroblast cell lines with a range of inhibitor dilutions for 2 h. Hereafter, cells were washed three times with PBS and subsequently harvested by scraping in potassium phosphate buffer (25 mM K_2HPO_4/KH_2PO_4, pH 6.5, supplemented with 0.1% (v/v) Triton X-100 and protease inhibitor cocktail (Roche)). After determination of the protein concentration (BCA kit, Pierce), lysates were transferred to aliquots and frozen at −80 °C. All IC_{50} values were determined by replicating each assay twice in duplicate in two separate cell lines. Data were corrected for background fluorescence, then normalized to the untreated control condition and finally curve-fitted with one-phase exponential decay function (GraphPad Prism 5.0). The kinetic parameters of inhibition were determined by adding rGBA, rGLA or rFUCA to the appropriate McIlvaine buffer, containing both substrate and various concentrations of the corresponding ABP. The mixture was incubated for 0 to 60 min at 37 °C and the reaction was stopped at intervals of 5 min with excess NaOH/glycine (pH 10.6). Inhibitory constants k_i and K_i' were determined by calculating the $K_{obs.}$ per ABP concentration and curve-fitting the data to a one-phase exponential association function (GraphPad Prism 5.0).[8a,9–11]

In vitro labeling and SDS-PAGE analysis

All pre-incubations and ABP labeling reactions occurred for 30 min at 37 °C, unless stated otherwise. The detection limit of each ABP was analyzed by labeling rGBA (10 pmol), rGLA (10 pmol) or rFUCA (100 μg total protein in lysate of COS-7 cells over-expressing rFUCA1) with 10000–0.01 nM ABP (**1**/**2**, **3**/**4**, **5**/**6**, respectively) for 30 min at 37 °C. Influence of pH on ABP labeling involved pre-incubation of the aforementioned enzyme/lysate at pH 3–10 for 30 min on ice, prior to addition of 100 nM ABP **1**/**2**, 1 μM ABP **3**/**4**/**5** or 10 μM ABP **6**, dissolved in Nanopure H_2O and incubation for 30 min at 37 °C. Assessment of ABP labeling kinetics involved pre-cooling of the enzyme mixture (100 fmol rGBA, 10 pmol rGLA, 10 μg total protein in lysate of COS-7 cells over-expressing rFUCA1, all dissolved in appropriate McIlvaine buffer) on ice for 15 min, followed by addition of similarly cooled ABP solution (100 fmol ABP **1**/**2**, 10 pmol ABP **3**/**4** or 10 μM ABP **5**/**6**, all dissolved in Nanopure H_2O). After mixing, ABP labeling was chased for 0–30 min, after which labeling was stopped by denaturation. For ABPP, rGBA (10 pmol), rGLA (10 pmol) or rFUCA (100 μg total protein in lysate of COS-7 cells over-expressing rFUCA1), or 100 μg total protein in lysate of human, wild-type GBA/GLA/FUCA1 fibroblasts, was pre-incubated with compounds 10 mM AMP/DNM, 1 mM CBE, 100 μM JJB339, JJB103, LWA481, LWA468, JJB349, JJB261 and LWA237, or boiled for 4 min in 2% (w/v) SDS, prior to labeling with 100 nM ABP **1**/**2**, 1 μM ABP **3**/**4**/**5** or 10 μM ABP **6** (all dissolved in Nanopure H_2O) for 30 min at 37 °C. Stability of the ABP–nucleophile adduct was analyzed by firstly labeling the various enzyme mixtures with the corresponding ABPs at appropriate McIlvaine conditions, after which the mixture was washed over Zeba spin desalting columns with 40 K MWCO resin, according to the manufacturer's instructions (Thermo Scientific). The eluted sample was separated, with 50% being snap-frozen in liquid nitrogen and stored at −20 °C, whereas the remaining 50% was chased for 8 h, including hourly washing with the appropriate McIlvaine buffer, over a new Zeba column. Samples were denatured with 5× Laemmli buffer (50% (v/v) 1 M Tris-HCl, pH 6.8, 50% (v/v) 100% glycerol, 10% (w/v) DTT, 10% (w/v) SDS, 0.01% (w/v) bromophenol blue), boiled for 4 min at 100 °C, and separated by gel electrophoresis on 10% (w/v) SDS-PAGE gels running continuously at 90 V.[8a,9–11] Wet slab-gels were then scanned for ABP-emitted fluorescence using a Typhoon TRIO variable mode imager (Amersham Biosciences) using $\lambda_{EX}=532$ nm and $\lambda_{EM}=610$ nM (band pass filter 30 nm) for red fluorescent ABPs **1**–**6**.

Acknowledgements

The China Scholarship Council (CSC Grant, to J.-B.J.) and the European Research Council (ERC AdG, to H.S.O.) are acknowledged for financial support.

Keywords: activity-based protein profiling · aziridine · biological activity · chemical biology · glycosidases

[1] a) D. J. Vocadlo, G. J. Davies, R. Laine, S. G. Withers, *Nature* **2001**, *412*, 835–838; b) D. L. Zechel, S. G. Withers, *Acc. Chem. Res.* **2000**, *33*, 11–18; c) G. Davies, B. Henrissat, *Structure* **1995**, *3*, 853–859.

[2] D. E. Koshland, *Biol. Rev.* **1953**, *28*, 416–436.

[3] a) K. A. Stubbs, *Carbohydr. Res.* **2014**, *390*, 9–19; b) L. I. Willems, J. Jiang, K. Y. Li, M. D. Witte, W. W. Kallemeijn, T. J. Beenakker, S. P. Schroder, J. M. Aerts, G. A. van der Marel, J. D. Codee, H. S. Overkleeft, *Chem. Eur. J.* **2014**, *20*, 10864–10872; c) B. F. Cravatt, A. T. Wright, J. W. Kozarich, *Annu. Rev. Biochem.* **2008**, *77*, 383–414.

[4] a) D. J. Vocadlo, C. R. Bertozzi, *Angew. Chem. Int. Ed.* **2004**, *43*, 5338–5342; *Angew. Chem.* **2004**, *116*, 5452–5456; b) K. A. Stubbs, A. Scaffidi, A. W. Debowski, B. L. Mark, R. V. Stick, D. J. Vocadlo, *J. Am. Chem. Soc.* **2008**, *130*, 327–335; c) O. Hekmat, Y.-W. Kim, S. J. Williams, S. He, S. G. Withers, *J. Biol. Chem.* **2005**, *280*, 35126–35135; d) J. D. McCarter, S. G. Withers, *J. Am. Chem. Soc.* **1996**, *118*, 241–242; e) B. P. Rempel, S. G. Withers, *Glycobiology* **2008**, *18*, 570–586.

[5] a) S. Atsumi, K. Umezawa, H. Iinuma, H. Naganawa, H. Nakamura, Y. Iitaka, T. Takeuchi, *J. Antibiot.* **1990**, *43*, 49–53; b) S. Atsumi, H. Iinuma, C. Nosaka, K. Umezawa, *J. Antibiot.* **1990**, *43*, 1579–1585.

[6] M. D. Witte, W. W. Kallemeijn, J. Aten, K.-Y. Li, A. Strijland, W. E. Donker-Koopman, A. M. C. H. van den Nieuwendijk, B. Bleijlevens, G. Kramer, B. I. Florea, B. Hooibrink, C. E. M. Hollak, R. Ottenhoff, R. G. Boot, G. A. van der Marel, H. S. Overkleeft, J. M. F. G. Aerts, *Nat. Chem. Biol.* **2010**, *6*, 907–913.

[7] V. Lombard, H. Golaconda Ramulu, E. Drula, P. M. Coutinho, B. Henrissat, *Nucleic Acids Res.* **2014**, *42*, D490–D495.

[8] a) M. D. Witte, M. T. Walvoort, K. Y. Li, W. W. Kallemeijn, W. E. Donker-Koopman, R. G. Boot, J. M. Aerts, J. D. Codee, G. A. van der Marel, H. S. Overkleeft, *ChemBioChem* **2011**, *12*, 1263–1269; b) M. T. Walvoort, W. W. Kallemeijn, L. I. Willems, M. D. Witte, J. M. Aerts, G. A. van der Marel, J. D. Codée, H. S. Overkleeft, *Chem. Commun.* **2012**, *48*, 10386–10388.

[9] a) W. W. Kallemeijn, K. Y. Li, M. D. Witte, A. R. Marques, J. Aten, S. Scheij, J. Jiang, L. I. Willems, T. M. Voorn-Brouwer, C. P. van Roomen, R. Ottenhoff, R. G. Boot, H. van den Elst, M. T. Walvoort, B. I. Florea, J. D. Codee, G. A. van der Marel, J. M. Aerts, H. S. Overkleeft, *Angew. Chem. Int. Ed.* **2012**, *51*, 12529–12533; *Angew. Chem.* **2012**, *124*, 12697–12701; b) B. Chandrasekar, T. Colby, A. Emran Khan Emon, J. Jiang, T. N. Hong, J. G. Villamor, A. Harzen, H. S. Overkleeft, R. A. van der Hoorn, *Mol. Cell. Proteomics* **2014**, *13*, 2787–2800.

[10] L. I. Willems, T. J. M. Beenakker, B. Murray, S. Scheij, W. W. Kallemeijn, R. G. Boot, M. Verhoek, W. E. Donker-Koopman, M. J. Ferraz, E. R. van Rijssel, B. I. Florea, J. D. C. Codee, G. A. van der Marel, J. M. F. G. Aerts, H. S. Overkleeft, *J. Am. Chem. Soc.* **2014**, *136*, 11622–11625.

[11] J. Jiang, W. W. Kallemeijn, D. W. Wright, A. M. C. H. van den Nieuwendijk, V. C. Rohde, E. C. Folch, H. van den Elst, B. I. Florea, S. Scheij, W. E. Donker-Koopman, M. Verhoek, N. Li, M. Schurmann, D. Mink, R. G. Boot, J. D. C. Codee, G. A. van der Marel, G. J. Davies, J. M. F. G. Aerts, H. S. Overkleeft, *Chem. Sci.* **2015**, *6*, 2782–2789.

[12] a) K. Tatsuta, Y. Niwata, K. Umezawa, K. Toshima, M. Nakata, *J. Antibiot.* **1991**, *44*, 912–914; b) M. Nakata, C. Chong, Y. Niwata, K. Toshima, K.

Tatsuta, *J. Antibiot.* **1993**, *46*, 1919 – 1922; c) K. Tatsuta, *Pure Appl. Chem.* **1996**, *68*, 1341 – 1346.

[13] K. Y. Li, J. B. Jiang, M. D. Witte, W. W. Kallemeijn, W. E. Donker-Koopman, R. G. Boot, J. M. F. G. Aerts, J. D. C. Codee, G. A. van der Marel, H. S. Overkleeft, *Org. Biomol. Chem.* **2014**, *12*, 7786 – 7791.

[14] a) K. Y. Li, J. B. Jiang, M. D. Witte, W. W. Kallemeijn, H. van den Elst, C. S. Wong, S. D. Chander, S. Hoogendoorn, T. J. M. Beenakker, J. D. C. Codee, J. M. F. G. Aerts, G. A. van der Marel, H. S. Overkleeft, *Eur. J. Org. Chem.* **2014**, 6030 – 6043; b) L. I. Willems, T. J. M. Beenakker, B. Murray, B. Gagestein, H. van den Elst, E. R. van Rijssel, J. D. C. Codée, W. W. Kallemeijn, J. M. F. G. Aerts, G. A. van der Marel, H. S. Overkleeft, *Eur. J. Org. Chem.* **2014**, 6044 – 6056.

[15] T. Wennekes, R. J. van den Berg, W. Donker, G. A. van der Marel, A. Strijland, J. M. Aerts, H. S. Overkleeft, *J. Org. Chem.* **2007**, *72*, 1088 – 1097.

Received: April 2, 2015
Published online on ■■ ■■, 0000

FULL PAPER

Chemical Biology

*J. Jiang, T. J. M. Beenakker, W. W. Kallemeijn, G. A. van der Marel, H. van den Elst, J. D. C. Codée, J. M. F. G. Aerts, H. S. Overkleeft**

■■ – ■■

Comparing Cyclophellitol *N*-Alkyl and *N*-Acyl Cyclophellitol Aziridines as Activity-Based Glycosidase Probes

N-acyl aziridine glycosidase ABP

N-alkyl ziridine glycosidase ABP

Taking the challenge: Development of cyclophellitol alkyl aziridine activity-based probes (ABPs) for labeling GH1 β-glucosidase, GH27 α-galactosidase and GH29 α-fucosidase is described. These ABPs were compared with the corresponding acyl ABPs (see figure).